

Molecular Geometry as a Source of Chemical Information. 5. Substituent Effect on Proton Transfer in Para-Substituted Phenol Complexes with Fluoride—a B3LYP/6-311+G** Study

Tadeusz M. Krygowski,[†] Halina Szatyłowicz,^{*,‡} and Joanna E. Zachara[†]

Department of Chemistry, Warsaw University, Pasteura 1, 02-093 Warsaw, Poland, and Faculty of Chemistry, Warsaw University of Technology, Noakowskiego 3, 00-664 Warsaw, Poland

Received December 6, 2004

The simplified model system $[p\text{-X-PhO}\cdots\text{H}\cdots\text{F}]^-$, where X are $-\text{NO}$, $-\text{NO}_2$, $-\text{CHO}$, $-\text{H}$, $-\text{CH}_3$, $-\text{OCH}_3$, and $-\text{OH}$, with various $\text{O}\cdots\text{F}$ distance was used to simulate the wide range of the H-bond strength. Structural changes due to variation of the substituent as well as the H-bond strength are well monitored by the changes in the aromaticity index HOMA and by two empirical measures of the H-bond strength—the ^1H NMR chemical shift of proton involved and the $\text{C}-\text{O}$ bond length. Changes in H-bonding strengths and the position of proton transfer while shortening the $\text{O}\cdots\text{F}$ distance are well described by the Hammett equation.

INTRODUCTION

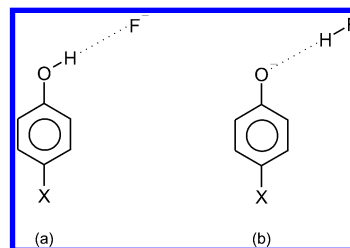
Substituent effects are classically referred to as kinetic, equilibrium state, and spectroscopic properties of cyclic π -electron systems, mostly to benzene or benzene-like systems.^{1–5} In this aspect geometric patterns have been less frequently studied.^{6–9} However, recently the geometry-based aromaticity index HOMA^{10,11} was used to study the changes in π -electron delocalization in the ring of monosubstituted benzenes¹² and H-bonded complexes of phenol derivatives with various bases¹³ or model complex with fluoride.¹⁴ Following the Hellmann–Feynman theorem,^{15,16} the distribution of electronic density in the molecule (or any chemical entity) determines the forces acting on the nuclei, which in turn defines the geometry of the molecule in question. Thus the geometry provides important information about electron distribution, and hence the studies of the substituent effects on the geometry of molecular moieties are well-founded.

Phenol and its derivatives exhibit substantial changes in their Brönsted acidity. Their $\text{p}K_{\text{a}}$ values vary from 0.71 for 2,4,6-trinitrophenol up to 12.23 for 2,6-di-*tert*-butyl-4-methylphenol.¹⁷ This range of $\text{p}K_{\text{a}}$ may be related to the strength of H-bond,^{18,19} particularly if the base in the complexes is fixed.¹³ That is why numerous studies can be found dealing with phenol derivatives used as model systems for the presentation of some attributes of the H-bond.^{20–25}

H-bonding is one of the most intensively and extensively studied kind of chemical interactions. It has been recognized in many phenomena in nature and has been studied from various points of view.^{26–30}

Recently phenol and its para-nitro derivative complexes with fluoride have been applied as model systems for studying the distant consequences of the H-bond formation

Chart 1



and its strength on π -electron delocalization in the ring.¹⁴ The changes in geometry of the studied complexes were found to be substantial. When a fluoride approaches the $-\text{OH}$ group in the phenols in question (Chart 1), then proton transfer is observed from the vicinity of the oxygen to F^- at a particular $\text{O}\cdots\text{F}$ distance varying with the para-substituent ($-\text{NO}_2$ and $-\text{H}$). It was found that the $\text{O}\cdots\text{F}$ distance for proton transfer is longer for the *p*-nitrophenol complex than for phenol, with the values equal to 2.601 and 2.503 Å, respectively.

The aim of this report is to analyze how para-substituents in phenol derivatives influence the value of $\text{O}\cdots\text{F}$ distance for proton transfer, the strength and geometry of the H-bond, and the changes in π -electron delocalization in the phenol ring.

METHODOLOGY

To simulate the wide range of the H-bond strength the simplified model system $[p\text{-X-PhO}\cdots\text{H}\cdots\text{F}]^-$ with various $\text{O}\cdots\text{F}$ distances was used, where X are $-\text{NO}$, $-\text{NO}_2$, $-\text{CHO}$, $-\text{H}$, $-\text{CH}_3$, $-\text{OCH}_3$, and $-\text{OH}$. Ab initio modeling at B3LYP level of theory and 6-311+G** basis set was applied to optimize the geometries of single molecules and H-bond complexes. In this model, the fluoride approaches the molecule of *p*-X-phenol along the line of prolongation of $\text{O}-\text{H}$ bond direction, as shown in Chart 1. The $\text{O}\cdots\text{F}$ distance is controlled, and the linearity of $\text{O}\cdots\text{H}\cdots\text{F}$ and the planarity of phenol ring are assumed. For the *p*-X-

* Corresponding author phone: +48 22 660 77 55; fax: +48 22 628 27 41; e-mail: halina@chemix.ch.pw.edu.pl.

[†] Warsaw University.

[‡] Warsaw University of Technology.

PhOH...F⁻ complexes the O...F distance was varied from 4.0 Å up to the distance when proton transfer from phenol to F⁻ was observed. For the same range of O...F distances the *p*-X-PhO⁻...HF complexes were optimized. Moreover, the optimal geometries of the [*p*-X-PhO...H...F]⁻ complexes (unconstrained O...F distance), *p*-X-phenols, and *p*-X-phenolates were calculated.

¹H NMR shifts were computed using the GIAO method. All the ab initio calculations were performed using Gaussian98.³¹

Bond lengths of phenol rings were used to calculate the values of aromaticity index HOMA^{32,33} according to the equation

$$\text{HOMA} = 1 - \frac{\alpha}{n} \sum (R_{\text{opt}} - R_i)^2 \quad (1)$$

where *n* is the number of bonds taken into the summation; α is a normalization constant (for CC bonds α = 257.7) fixed to give HOMA = 0 for a model nonaromatic system, e.g. Kekulé structure of benzene³⁴ and HOMA = 1 for the system with all bonds equal to the optimal value *R*_{opt} assumed to be realized for full aromatic systems (for CC bonds *R*_{opt} is equal to 1.388 Å); and *R*_{*i*} stands for a running bond length. For wide applications and limitation of the HOMA index, see refs 11 and 35.

RESULTS AND DISCUSSION

Analyses of H-bond complexes (Chart 1, -X = -NO, -NO₂, -CHO, -H, -CH₃, -OCH₃, and -OH) and substituent effect are considered for several model situations:

- (i) the para substituted phenol derivatives,
- (ii) the optimal structures of [*p*-X-PhO...H...F]⁻,
- (iii) *p*-X-PhOH...F⁻ complexes for various O...F distances between 4.0 Å and the value of proton transfer (pt),
- (iv) *p*-X-PhO⁻...HF complexes for various O...F distances between 4.0 Å and the distance at which in (iii) proton transfer was observed.

The difference between the *p*-X-PhOH...F⁻ and *p*-X-PhO⁻...HF complexes is associated with a different behavior of proton while decreasing the O...F distance. In the case of *p*-X-PhOH...F⁻ at a particular O...F distance (pt) the proton transfer from oxygen to fluoride takes place. It is not observed in the other case.¹⁴

Table 1a,b presents selected geometry parameters for *p*-X-phenols, *p*-X-phenolates, and [*p*-X-PhO...H...F]⁻ complexes that are important for further discussion.

It was shown that the C-O bond length is the most varying structural parameter in the case of PhOH...Base interactions.³⁷ The variation in the C-O bond length for phenol and [*p*-X-PhO...H...F]⁻ as well as the O...H distance follows the Hammett rule (Figures 1 and 2, respectively). Obviously, the stronger the electron donating group (-OH, -O...HF) is, the steeper slope is found, as shown in Figures 1 and 2. It is worth mentioning that in all optimal structures the proton is located at the fluoride.

Note that in the case of the O-H bond lengths (Figure 2), their variation for phenol derivatives is very small but also follows the Hammett equation.^{1,36} The O...H distance for the equilibrium complex [*p*-X-PhO...H...F]⁻ is the most flexible one of the discussed parameters—but in this case it is not a covalent bond but the O...H contact. Definitely the

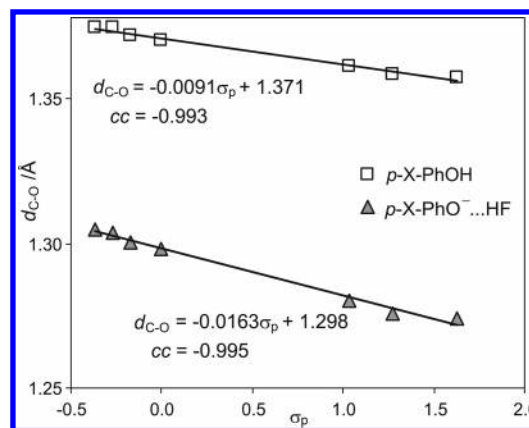


Figure 1. Dependences of the C-O bond length, *d*_{C-O}, in *p*-X-PhOH and optimal structures of [*p*-X-PhO...H...F]⁻ on a substituent constant, σ_p (for electron accepting substituents σ_p⁻ are used).

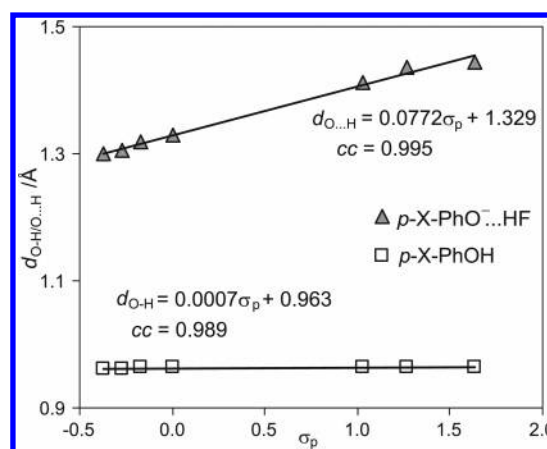


Figure 2. Dependences of the O-H bond length, *d*_{O-H}, and the O...H contact, *d*_{O...H}, in *p*-X-PhOH and optimal structures of [*p*-X-PhO...H...F]⁻, respectively, on a substituent constant, σ_p (for electron accepting substituents σ_p⁻ are used).

force constants for this case are much smaller, and hence deformations are energetically cheaper.

The substituent effect also decides about the behavior of a proton in the space between oxygen and fluoride when the O...F distance is decreased. The distance when proton transfer is realized characterizes the energetic situation of the proton placed between two negatively charged entities. It is not possible to estimate the distance for the transfer itself, but only the distance just before or after the transfer. In our case we have taken into account the second situation. Figure 3 presents the dependence of the O...F distance for proton transfer of [*p*-X-PhO...H...F]⁻ complexes on Hammett's substituent constants.

The stronger the electron-withdrawing power of the substituent is, the longer the O...F distance for proton transfer is. This is due to the through resonance effect. When the charge on the oxygen atom becomes less negative, then proton transfer is facilitated from *p*-X-PhOH...F⁻ to *p*-X-PhO⁻...HF.

There is also a more complex problem of long-distance consequences of H-bonding expressed by the changes in π-electron delocalization in the ring as well as interrelations between some measures of the H-bond strength.

The analysis of the variation of the HOMA index in three groups of data presented in Table 1 (for substituted phenols,

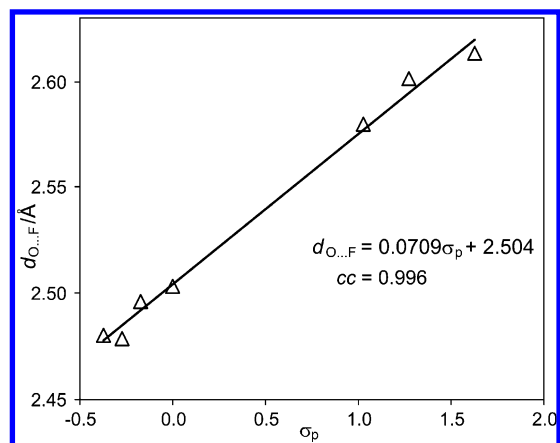


Figure 3. Dependence of the O...F distance for proton transfer, $d_{O...F}$, for $[p\text{-X-PhO}\cdots\text{H}\cdots\text{F}]^-$ complexes on a substituent constant, σ_p (for electron accepting substituents σ_p^- are used).

Table 1.

a. C–O and O–H Bond Lengths (d_{C-O} , d_{O-H}), HOMA Values, and Substituent Constants,³⁶ σ_p , for Phenols and Phenolates

molecule	σ_p	$d_{C-O}/\text{\AA}$	$d_{O-H}/\text{\AA}$	HOMA
<i>p</i> -NO-phenol	1.63 ^a	1.357	0.964	0.963
<i>p</i> -NO ₂ -phenol	1.27 ^a	1.358	0.964	0.985
<i>p</i> -CHO-phenol	1.03 ^a	1.361	0.964	0.969
phenol	0.00	1.370	0.963	0.989
<i>p</i> -CH ₃ -phenol	−0.17	1.372	0.963	0.984
<i>p</i> -OCH ₃ -phenol	−0.27	1.374	0.962	0.981
<i>p</i> -OH-phenol	−0.37	1.374	0.962	0.989
<i>p</i> -NO-phenolate	1.63 ^a	1.252		0.410
<i>p</i> -NO ₂ -phenolate	1.27 ^a	1.253		0.514
<i>p</i> -CHO-phenolate	1.03 ^a	1.257		0.500
phenolate	0.00	1.269		0.683
<i>p</i> -CH ₃ -phenolate	−0.17	1.271		0.698
<i>p</i> -OCH ₃ -phenolate	−0.27	1.273		0.729
<i>p</i> -OH-phenolate	−0.37	1.273		0.733

b. C–O and O...H Interatomic Distances (d_{C-O} , $d_{O...H}$), HOMA Values, Substituent Constants,³⁶ σ_p , and the O...F Distance ($d_{O...F}$) for the Optimal $p\text{-X-PhO}\cdots\text{H}\cdots\text{F}$ Complexes and for Proton Transfer

complex	σ_p	$d_{C-O}/\text{\AA}$	$d_{O...H}/\text{\AA}$	HOMA	$d_{O...F}/\text{\AA}$	
					optimal	proton transfer
<i>p</i> -NO-PhO [−] ...HF	1.63 ^a	1.274	1.445	0.630	2.445	2.613
<i>p</i> -NO ₂ -PhO [−] ...HF	1.27 ^a	1.276	1.437	0.717	2.445	2.601
<i>p</i> -CHO-PhO [−] ...HF	1.03 ^a	1.280	1.413	0.707	2.425	2.580
PhO [−] ...HF	0.00	1.298	1.328	0.855	2.382	2.503
<i>p</i> -CH ₃ -PhO [−] ...HF	−0.17	1.300	1.321	0.864	2.379	2.496
<i>p</i> -OCH ₃ -PhO [−] ...HF	−0.27	1.304	1.305	0.888	2.372	2.479
<i>p</i> -OH-PhO [−] ...HF	−0.37	1.305	1.299	0.891	2.370	2.480

^a For electron accepting substituents σ_p^- are used.

phenolates, and complexes $[p\text{-X-PhO}\cdots\text{H}\cdots\text{F}]^-$ reveals that in the case of phenols the range of changes in HOMA is very small, of about 0.03 unit; for phenolates this range is 0.32, whereas for the complex it is equal to 0.26. Evidently, the strong electron donating oxygen in phenolates causes strong changes in aromaticity of the ring when the counter substituent is electron withdrawing. The same is true for the complexes. Figure 4a presents the changes in HOMA for all the complexes (cases iii and iv) plotted against the C–O bond length, used here as a measure of H-bond strength.³⁷ The shape of the changes in HOMA in Figure 4a is qualitatively the same as that observed¹³ for X-ray data³⁸ (Figure 4b). To show how much the HOMA values depend

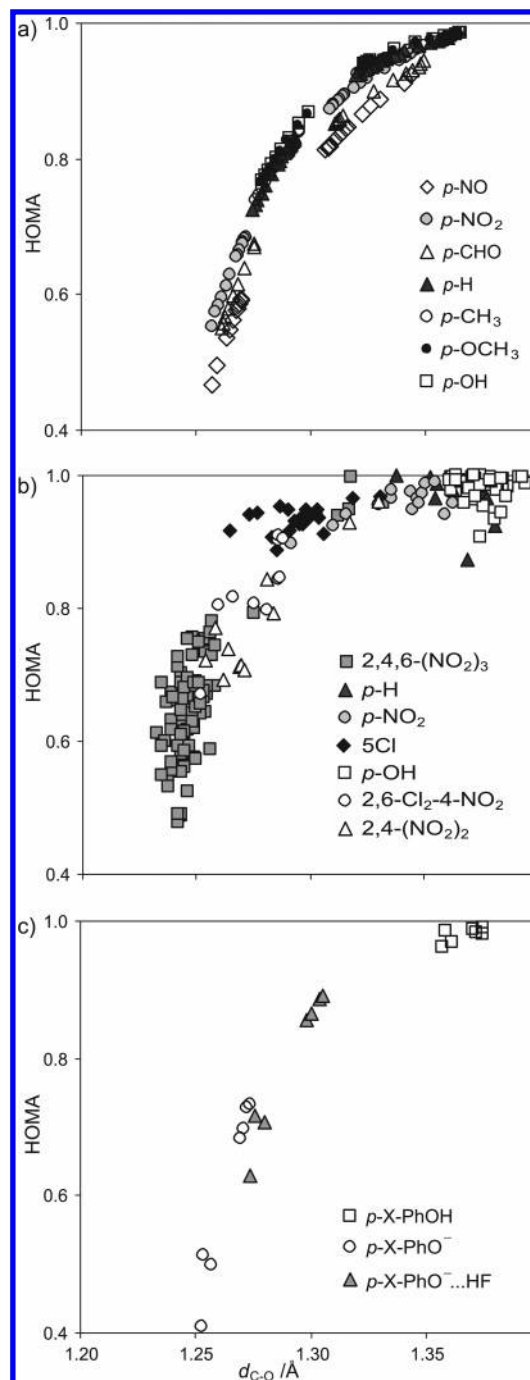


Figure 4. Dependence of HOMA on the C–O bond length, d_{C-O} , for (a) $[p\text{-X-PhO}\cdots\text{H}\cdots\text{F}]^-$ complexes, (b) 7 types of substituted phenols¹³ (X-ray data), and (c) phenols, phenolates, and optimal complexes $[p\text{-X-PhO}\cdots\text{H}\cdots\text{F}]^-$.

on the H-bond strength in the limiting cases— $p\text{-X-PhOH}$, $p\text{-X-PhO}^-$, and optimal complexes $[p\text{-X-PhO}\cdots\text{H}\cdots\text{F}]^-$ —Figure 4c presents the appropriate scatter plots.

For cases (iii) and (iv) another analysis was carried out. The changes in the C–O bond length may be used as a measure of the H-bond strength for $p\text{-X-PhOH}\cdots\text{F}^-$ and $p\text{-X-PhO}^- \cdots \text{HF}$ complexes.³⁷ It is known that another useful, empirical measure of the H-bond strength is frequently applied—the ¹H NMR chemical shift of the proton in the H-bond.^{27,39,40} Figure 5 presents a mutual dependence of these two measures of the H-bond strength for the cases when for *p*-substituted systems the O...F distance was varied

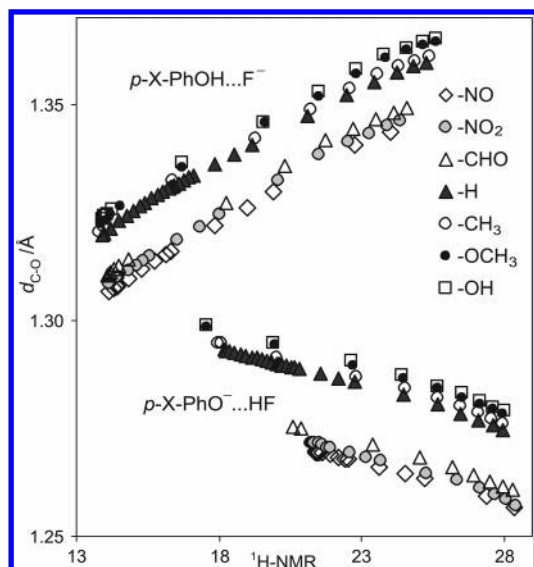


Figure 5. Dependence of two empirical measures of H-bond strengths: the ^1H NMR chemical shift of the proton involved and the C–O bond length, $d_{\text{C-O}}$, for $[p\text{-X-PhO}\cdots\text{H}\cdots\text{F}]^-$ complexes.

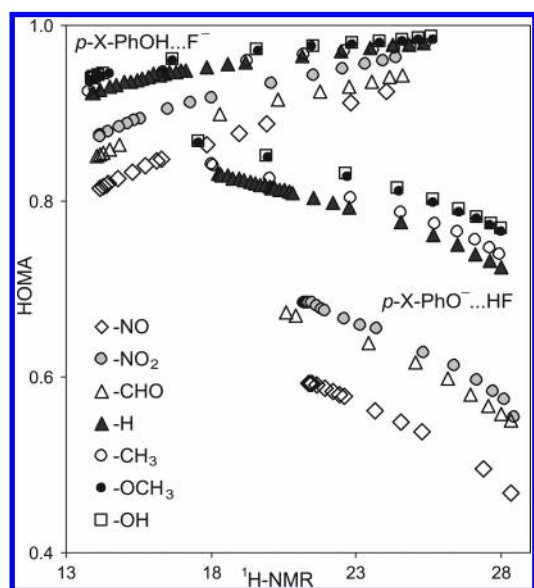


Figure 6. Dependence of the HOMA value on the ^1H NMR chemical shift of the proton involved for $[p\text{-X-PhO}\cdots\text{H}\cdots\text{F}]^-$ complexes.

leading to the changes in the properties of the H-bond (its strength) and in the geometry of the ring. The linear correlations for $p\text{-X-PhOH}\cdots\text{F}^-$ and $p\text{-X-PhO}\cdots\text{HF}$ complexes are excellent—the absolute values of the correlation coefficients for these regressions are always above 0.99. This indicates nicely a very good equivalence between the two measures of the H-bond strength, at least for these kinds of systems.

Figure 6 presents the dependences of π -electron delocalization for $p\text{-X-PhOH}\cdots\text{F}^-$ and $p\text{-X-PhO}\cdots\text{HF}$ described by the HOMA index on the strength of the H-bond approximated by ^1H NMR shifts.

The positively inclined parts of the scatter plots are for $p\text{-X-PhOH}\cdots\text{F}^-$ complexes, whereas those with negative slopes are for $p\text{-X-PhO}\cdots\text{HF}$. Clearly, the stronger the electron withdrawing power of the substituent is, the lower HOMA is. When fluoride approaches the $-\text{OH}$ group, the H-bond becomes stronger, which causes a lower ^1H NMR

Table 2. Slopes, s , of the Regression Lines of HOMA Values vs ^1H NMR for $[p\text{-X-PhO}\cdots\text{H}\cdots\text{F}]^-$ Complexes, Correlation Coefficient, cc , and Substituent Constant,³⁶ σ_p

substituent	$p\text{-X-PhOH}\cdots\text{F}^-$		$p\text{-X-PhO}\cdots\text{F}$		σ_p
	s	cc	s	cc	
–NO	0.0112	0.994	–0.0172	–0.994	1.63 ^a
–NO ₂	0.0085	0.993	–0.0161	–0.992	1.27 ^a
–CHO	0.0088	0.996	–0.0158	–0.993	1.03 ^a
–H	0.0046	0.978	–0.0103	–0.994	0.00
–CH ₃	0.0044	0.979	–0.0097	–0.991	–0.17
–OCH ₃	0.0041	0.983	–0.0096	–0.993	–0.27
–OH	0.0039	0.985	–0.0094	–0.992	–0.37

^a For electron accepting substituents σ_p^- are used.

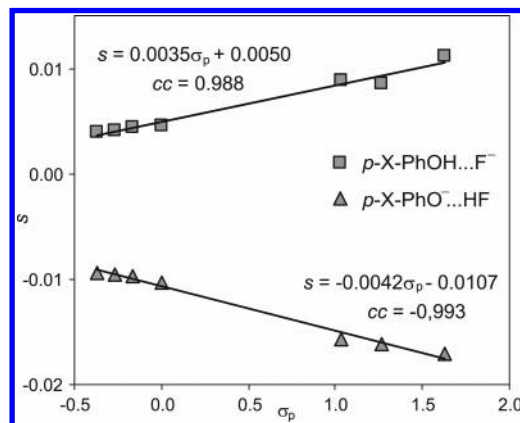


Figure 7. Relation between the slopes, s , of the regression line of the HOMA values vs ^1H NMR for the $[p\text{-X-PhO}\cdots\text{H}\cdots\text{F}]^-$ complexes and substituent constants, σ_p (for electron accepting substituents σ_p^- are used).

chemical shift. A very similar situation is observed for the case of $p\text{-X-PhO}\cdots\text{HF}$ complexes: the approach of HF to the $p\text{-X-phenolate}$ anion causes an increase of the H-bond strength, and thus a decrease of the ^1H NMR shift follows. The reverse sequence of dependences for $-\text{NO}_2$ and $-\text{CHO}$ shown in Figure 6 than it would result from σ_p^- values (1.27 and 1.03, respectively) is a consequence of internal resonance effect in the nitro group and its lack for the formyl one.

In general, the stronger the electron withdrawing power of the substituent is, the less negative the oxygen atom is, and hence the $p\text{-X-PhO}\cdots\text{HF}$ interaction is generally weaker than in the case of $p\text{-X-PhOH}\cdots\text{F}^-$. The dependences of the HOMA values on the ^1H NMR shifts may be approximated by linear regressions, as it results from scatter plots in Figure 6. The regression lines obtained differ not only in their position on the ^1H NMR chemical shift axis but also in their slopes. Table 2 presents those data.

The slopes of the dependences of HOMA values for $p\text{-X-PhO}\cdots\text{HF}$ and $p\text{-X-PhOH}\cdots\text{F}^-$ complexes on the ^1H NMR chemical shift represent the sensitivity of the π -electron delocalization in the ring on the strength of the H-bond. The slopes depend on the substituent constant, as shown in Figure 7.

The slopes in Figure 7 indicate a regularity—the stronger the electron accepting substituent is the greater the sensitivity is of dependences presented in Figure 6. This may be interpreted as follows. The $\text{O}\cdots\text{H}\cdots\text{F}$ moiety is always an electron donating entity with its donicity dependent on the H-bond strength. The electron withdrawing substituent in the para position acts always in a way to induce a quinoid-like

structure exhibiting a strong cooperative effect realized by a partial charge transfer to the substituent. Therefore for substituents such as $-\text{NO}$, $-\text{CHO}$, and $-\text{NO}_2$ the slopes in Figure 6 (Table 2) are the largest. In the case of electron donating substituents the situation is opposite.

CONCLUSIONS

It results from the study that structural changes due to variation of the substituent as well as the H-bond strength are well monitored by the changes in the aromaticity index HOMA and by two empirical measures of the H-bond strength—the ^1H NMR chemical shift of the proton involved and the C—O bond length.

A general conclusion is that the quantities characterizing H-bonding strengths linearly depend on the Hammett substituent constants³⁶ σ_p and σ_p^- (for electron accepting substituents). The distant structural consequences of H-bonding depend on its strength.

ACKNOWLEDGMENT

The authors thank the Interdisciplinary Center for Mathematical and Computational Modeling (Warsaw, Poland) for computational facilities.

REFERENCES AND NOTES

- Hammett, L. P. *Physical Organic Chemistry*; McGraw-Hill: New York, 1st ed. 1940; 2nd ed. 1970.
- Jaffe, H. H. A Reexamination of the Hammett Equation. *Chem. Rev.* **1953**, *53*, 191–261.
- Exner, O. In *Advances in Linear Free Energy Relationships*; Chapman, N. B., Shorter, J., Eds.; Plenum Press: London, 1972; Chapter 1, pp 1–69.
- Johnson, C. D. *The Hammett Equation*; Cambridge University Press: 1973.
- Shorter, J. In *Similarity Models in Organic Chemistry, Biochemistry and Related Fields*; Zalewski, R. I., Krygowski, T. M., Shorter, J., Eds.; Elsevier: Amsterdam, 1991; Chapter 2, pp 77–147.
- Domenicano, A.; Vaciagio, A.; Coulson, C. A. Molecular Geometry of Substituted Benzene Derivatives. Part 1. On the Nature of the Ring Deformations Induced by Substitution. *Acta Crystallogr.* **1975**, *B31*, 221–234.
- Domenicano, A.; Vaciagio, A.; Coulson, C. A. Molecular Geometry of Substituted Benzene Derivatives. II. A Bond Angle versus Electronegativity Correlation for the Phenyl Derivatives of Second-Row Elements. *Acta Crystallogr.* **1975**, *B31*, 1630–1641.
- Domenicano, A.; Murray-Rust, P. Geometrical Substituent Parameters for Benzene Derivatives: Inductive and Resonance Effects. *Tetrahedron Lett.* **1979**, 2283–2286.
- Krygowski, T. M. Crystallographic Studies and Physicochemical Properties of π -Electron Systems. Part 5. Substituent Effect on the Geometry of the Benzene Ring in Benzene Derivatives. *J. Chem. Res. (S)* **1984**, 238–239.
- Krygowski, T. M. Crystallographic Studies of Inter- and Intramolecular Interactions Reflected in Aromatic Character of π -Electron Systems. *J. Chem. Inf. Comput. Sci.* **1993**, *33*, 70–78.
- For review: Krygowski, T. M.; Cyrański, M. K. Structural Aspects of Aromaticity. *Chem. Rev.* **2001**, *101*, 1385–1419.
- Krygowski, T. M.; Ejsmont, K.; Stępień, B. T.; Cyrański, M. K.; Poater, J.; Sola M. Relation between the Substituent Effect and Aromaticity. *J. Org. Chem.* **2004**, *69*, 6634–6640.
- Krygowski, T. M.; Szatyłowicz, H.; Zachara, J. E. How H-Bonding Affects Aromaticity of the Ring in Various Substituted Phenol Complexes with Bases. 4. Molecular Geometry as a Source of Chemical Information. *J. Chem. Inf. Comput. Sci.* **2004**, *44*, 2077–2082.
- Krygowski, T. M.; Zachara, J. E.; Szatyłowicz, H. Molecular Geometry as a Source of Chemical Information. 3. How H-Bonding Affects Aromaticity of the Ring in the Case of Phenol and *p*-Nitrophenol Complexes: a B3LYP/6-311+G** Study. *J. Org. Chem.* **2004**, *69*, 7038–7043.
- Hellmann, H. *Einführung in die Quantenchemie*; Franz Deuticke, Leipzig, 1937.
- Feynman, R. P. Forces in Molecules. *Phys. Rev.* **1939**, *56*, 340–343.
- Kortum, G.; Vogel, W.; Andrussow, A. *Dissociation Constants of Organic Acids in Aqueous Solution*; Butterworth: London, 1961.
- Huyskens P.; Zeegers-Huyskens, T. Association Molaire et Equilibres Acide-Base. *J. Chim. Phys.* **1964**, *61*, 81–86.
- Huyskens, P.; Sobczyk, L.; Majerz, I. On a Hard/Soft Hydrogen Bond Interaction. *J. Mol. Struct.* **2002**, *615*, 61–72.
- Steiner, T.; Majerz, I.; Wilson, C. C. First O \cdots H \cdots N Hydrogen Bond with a Centered Proton Obtained by Thermally Induced Proton Migration. *Angew. Chem., Int. Ed. Engl.* **2001**, *40*, 2651–2654.
- Zierkiewicz, W.; Michalska, D.; Czarnik-Matusewicz, B.; Rospenk, M. Molecular Structures and Infrared Spectra of 4-Fluorophenol. A Combined Theoretical and Spectroscopic Study. *J. Phys. Chem. A* **2003**, *107*, 4547–4554.
- Korth, H.-G.; de Heer, M. I.; Mulder, P. A DFT on Intermolecular Hydrogen Bonding in 2-Substituted Phenols: Conformations, Enthalpies, and Correlation with Solute Parameters. *J. Phys. Chem. A* **2002**, *106*, 8779–8789.
- Mandado, M.; Mosquera, R. A.; Grana, A. M. AIM Interpretation of the Acidity of Phenol Derivatives. *Chem. Phys. Lett.* **2004**, *386*, 454–459.
- Sobczyk, L. X-ray Diffraction, IR, UV and NMR Studies on Proton-Transfer Equilibrating Phenol \cdots N \cdots Base Systems. *Ber. Bunsen. Phys. Chem.* **1998**, *102*, 377–383.
- Abkowitz-Bienko, A. J.; Latajka, Z.; Bienko, D. C.; Michalska D. Theoretical Infrared Spectrum and Revised Assignment for para-Nitrophenol. Density Functional Theory Studies. *Chem. Phys.* **1999**, *250*, 123–129.
- Jeffrey, G. A.; Saenger, W. *Hydrogen Bonding in Biological Structures*; Springer: Berlin, 1991.
- Jeffrey, G. A. *An Introduction to Hydrogen Bonding*; Oxford University Press: Oxford, 1997.
- Scheiner, S. *Hydrogen Bonding, A Theoretical Perspective*; Oxford University Press: Oxford, 1997.
- Desiraju, G. R.; Steiner, T. *The weak Hydrogen Bonding in Structural Chemistry and Biology*; Oxford University Press: Oxford, 1999.
- Steiner, T. The Hydrogen Bond in the Solid State. *Angew. Chem., Int. Ed. Engl.* **2002**, *41*, 48–76.
- Frisch, M. J.; Trucks, G. W.; Schlegel, H. B.; Scuseria, G. E.; Robb, M. A.; Cheeseman, J. R.; Zakrzewski, V. G.; Montgomery, J. A., Jr.; Stratmann, R. E.; Burant, J. C.; Dapprich, S.; Millam, J. M.; Daniels, A. D.; Kudin, K. N.; Strain, M. C.; Farkas, O.; Tomasi, J.; Barone, V.; Cossi, M.; Cammi, R.; Mennucci, B.; Pomelli, C.; Adamo, C.; Clifford, S.; Ochterski, J.; Petersson, G. A.; Ayala, P. Y.; Cui, Q.; Morokuma, K.; Malick, D. K.; Rabuck, A. D.; Raghavachari, K.; Foresman, J. B.; Cioslowski, J.; Ortiz, J. V.; Baboul, A. G.; Stefanov, B. B.; Liu, G.; Liashenko, A.; Piskorz, P.; Komaromi, I.; Gomperts, R.; Martin, R. L.; Fox, D. J.; Keith, T.; Al-Laham, M. A.; Peng, C. Y.; Nanayakkara, A.; Gonzalez, C.; Challacombe, M.; Gill, P. M. W.; Johnson, B.; Chen, W.; Wong, M. W.; Andres, J. L.; Gonzalez, C.; Head-Gordon, M.; Replogle, E. S.; Pople, J. A. *Gaussian 98; Revision A.7* Gaussian Inc.: Pittsburgh, PA, 1998.
- Kruszewski, J.; Krygowski, T. M. Definition of Aromaticity Basing on the Harmonic Oscillator Model. *Tetrahedron Lett.* **1972**, 3839–3842.
- Krygowski, T. M. Crystallographic Studies of Inter- and Intramolecular Interaction Reflected in Aromatic Character of π -Electron Systems. *J. Chem. Inf. Comput. Sci.* **1993**, *33*, 70–78.
- Julg, A.; Françoise, P. Geometry of Nonalternant Hydrocarbons: its Influence on the Transition Energies, a New Definition of Aromaticity. *Theor. Chim. Acta* **1967**, *8*, 249–259.
- Krygowski, T. M.; Cyrański, M. K. Two Faces of the Structural Aspects of Aromaticity. *Phys. Chem. Chem. Phys.* **2004**, *6*, 249–255.
- Hansch, C.; Leo, A.; Taft, W. A Survey of Hammett Substituent Constants and Resonance and Field Parameters. *Chem. Rev.* **1991**, *91*, 165–195.
- Krygowski, T. M.; Zachara, J. E.; Szatyłowicz, H. Molecular Geometry as a Source of Chemical Information. Part 2. An Attempt to Estimate the H-Bond Strength: the Case of *p*-Nitrophenol Complexes with Bases. *J. Phys. Org. Chem.* **2005**, *18*, 110–114.
- The Cambridge Structure Database, the 5.25 version, November 2003, updated January 2004.
- Schaeffer, T. A Relationship between Hydroxyl Proton Chemical Shifts and Torsional Frequencies in Some *ortho*-Substituted Phenol Derivatives. *J. Phys. Chem.* **1975**, *79*, 1888–1890.
- Bertolasi, V.; Gilli, P.; Ferretti, V.; Gilli, G. Intramolecular O—H \cdots O Hydrogen Bonds Assisted by Resonance. Correlation between Crystallographic Data and ^1H NMR Chemical Shifts. *J. Chem. Soc., Perkin Trans. 2* **1997**, 945–952.